Journal of Macromolecular Science, Part A
Publication details, including instructions for authors and subscription information:
http://www.informaworld.com/smpp/title~content=t713597274

The Structural Features of Low Molecular Weight Ionic Diblock Polymers Based on Group Transfer Polymerized Methacrylates

Don Loveday[a,b]; Garth L. Wilkes[a]
[a] Polymer Materials and Interfaces Laboratory Department of Chemical Engineering Virginia Polytechnic, Institute and State University Blacksburg, Virginia, USA [b] Exxon Chemical Company, Baytown Polymers Center, Baytown, TX

To cite this Article Loveday, Don and Wilkes, Garth L.(1997) 'The Structural Features of Low Molecular Weight Ionic Diblock Polymers Based on Group Transfer Polymerized Methacrylates', Journal of Macromolecular Science, Part A, 34: 5, 807 — 818

To link to this Article: DOI: 10.1080/10601329708014332

URL: http://dx.doi.org/10.1080/10601329708014332

J.M.S.—PURE APPL. CHEM., A34(5), pp. 807–818 (1997)

THE STRUCTURAL FEATURES OF LOW MOLECULAR WEIGHT IONIC DIBLOCK POLYMERS BASED ON GROUP TRANSFER POLYMERIZED METHACRYLATES

DON LOVEDAY† and GARTH L. WILKES*

Polymer Materials and Interfaces Laboratory
Department of Chemical Engineering
Virginia Polytechnic Institute and State University
Blacksburg, Virginia 24061-0211, USA

ABSTRACT

The solid-state ordered structures formed by low M_n ionic diblock copolymers of less than 10,000 g/mol, made by group-transfer polymerization of methacrylates, were studied. The unquaternized diblocks exhibit no structure via small-angle x-ray scattering (SAXS) and are apparently below their critical value of χN in a disordered melt state at room temperature. However, the amine salt ionomers exhibit morphologies ranging from dispersed spheres to lamellae which were investigated by SAXS and transmission electron microscopy (TEM). The morphology depends strongly on the size and proportion of the blocks, the extent of quaternization, and the concentration of the blocks in the casting solution.

---

†Present address: Exxon Chemical Company, Baytown Polymers Center, 5200 Bayway Drive, Baytown, TX 77520.

INTRODUCTION

Group transfer polymerization (GTP) has become a widely used polymerization technique for methacrylates since it was first reported in patents and papers by Webster, Sogah, and others [1]. A major advantage of GTP is that block copolymers of methacrylates may be obtained, which is difficult via traditional anionic methods without the use of protective groups [2]. The molecular weight distribution is relatively narrow for polymethacrylate block copolymers made by GTP and similar to that of anionically synthesized block copolymers, with a typical M_w/M_n of ≤ 1.2 [3]. Other architectures, such as combs, multi-armed stars, and star-blocks, have also been produced by the GTP method [4–8].

Small-angle x-ray scattering (SAXS) has been used for many years to study the development of ordered structures (or clustering) by small molecules in solution. Luzzati and Reiss-Husson studied the SAXS of salts of fatty acids in dilute and concentrated aqueous solutions [9]. These small molecules form spherical micellar structures at low concentrations or rodlike structures at high concentrations with a hydrophobic interior and a hydrophilic exterior. Such structures tend to exhibit greater shape anisotropy as the carbon—carbon "tail" of the molecule is lengthened, with a 9-carbon tail giving spherical micelles and a 15-carbon tail prolate ellipsoids. It was also shown that the number of micelles increased but their size decreased as the solution temperature increased. It is well-known that other small, amphoteric molecules form structures in solution, such as phospholipids [10]. These materials form the simplest membrane feature, the phospholipid bilayer, where the hydrophobic "tails" are internal and the hydrophilic "heads" are external. Such structures regulate the interchange of nutrients and gases between the cell (or a cellular structure) and the surrounding medium. SAXS studies of phospholipids indicate that they easily form multilamellar structures [11]. This structure-forming tendency of small molecules in solution is certainly an important and varied topic of study.

Ionic GTP block copolymers from methacrylates are used in several important applications such as in inks, antistatics, polymer-polymer compatibilization, and triboelectricity (development of an electrical field when rubbed). The morphology of relatively low M_n ionic diblock copolymers based on poly(benzyl methacrylate-*block*-dimethylaminoethyl methacrylate) is thus of interest. The premise of this study was that these short diblock ionomers might form highly ordered structures in the solid state. Such structures are favored due to the diblock character of these molecules, a relatively narrow MWD, and the phase separation often induced via ionization.

EXPERIMENTAL

The methacrylate diblock polymers used as precursors to the ionomers in this study were produced using an MTS/alkylammonium benzoate initiator/catalyst system. The polymerization technique is proprietary in nature, but is similar to MTS/nucleophile-catalyzed polymerizations [2, 3]. The materials were characterized in terms of MWD by size exclusion chromatography and have relatively narrow MWDs in each block and in the overall molecule (M_w/M_n ca. 1.2). These polymers were stored in 60/40 THF/isopropanol at ca. 50 wt% polymer until use. The un-

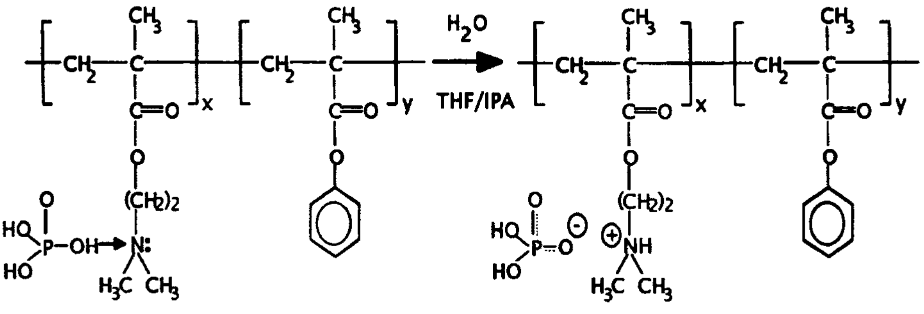

FIG. 1. Quaternization of BZ-DMAE copolymers with H_3PO_4, single dissociation. The numbers X//Y refer to the $\overline{X}_n$ of the BZ//DMAE blocks.

quaternized polymers were cast into silicone rubber molds and allowed to dry at 23 °C over the course of 2 weeks. The ionomers were made by adding an appropriate amount of 1 wt% H_3PO_4/water solution to the 60/40 THF/isopropanol polymer solution and vigorously shaking. This process of forming the 2-(dimethylammonium)ethyl ester (the amine salt) for a single dissociation of H_3PO_4 is illustrated schematically in Fig. 1.

After the formation of the amine salt, the 30 wt% polymer solutions were cast into covered silicone rubber molds and allowed to air dry at 23 °C for 2 weeks. No further drying was attempted, as preliminary results from small-angle x-ray scattering (SAXS) showed that the structural features of the system changed when dried at 100 °C under vacuum for 3 hours. Specifically, the multiple peaks observed in SAXS before oven drying were seen to become one large peak at lower angles after the drying step at higher temperature. As expected, all the plaques formed from either the unquaternized material or the ionomer were brittle and not structural materials. In Table 1 it is apparent that the maximum M_n in these materials, 12,760 g/mol, is

TABLE 1. Smeared SAXS Interdomain Spacings of the Diblock Ionomers from Bragg's Law

Diblock[a]	M_n, g/mol[b]	d_1, nm	d_2, nm	d_3, nm
10//40	8,050	11.3	4.5[c]	None
5//10	2,405	7.9	3.7	None
10//20	4,810	9.0	3.7	None
20//40	9,620	13.5	6.9	4.1[c]
20//20	6,380	12.7	7.1	4.5[c]
40//40	12,760	29.8	16.2	10

[a] Values are DP_n of the BZMA//DMAEMA diblock.

[b] Molecular weight determined from the DP_n of the BZMA//DMAEMA diblock.

[c] Denotes weak scattering peaks.

still too low to exhibit mechanical integrity. The nomenclature used is X//Y, where X is the DP_n of the benzyl methacrylate (BZ) block and Y is the DP_n of the dimethylaminoethyl methacrylate (DMAE) block. SAXS profiles were collected on a Kratky camera using Ni-filtered CuKα radiation (λ = 0.15418 nm) from a Philips PW-1729 generator. Wide-angle x-ray diffraction profiles were collected with a Nicolet diffractometer operating at 40 kV and 30 mA, equipped with a STOE Bragg-Brentano goniometer. TEM was done on a Philips STEM-610 at 60 kV using samples microtomed in hexamethyl disiloxane at 23°C.

RESULTS AND DISCUSSION

Effect of Block Length on Structure

Using GTP polymerization, fairly uniform molecular size and composition were obtained. By maintaining a 1:2 molar ratio of BZ and DMAE blocks and increasing the total length of the diblock, one considers the effect of molecular size alone. This is illustrated in Fig. 2, which shows the smeared SAXS profiles for 1:2 BZ//DMAE diblocks of 15, 30, and 60 total DP_n which were quaternized to 90% of the amine content (as in Fig. 1). In Fig. 2 the log of the scattered intensity is plotted versus the log of the scattering variable s, $s = (2/\lambda)\sin(\theta)$, where θ is one-half the radial scattering angle. The primary peak moves to lower angles and the intensity of the peak increases as the DP_n of the diblock ionomer increases from 15 to 60 units. The estimated interdomain spacing ($d \sim 1/s_{\text{peak}}$) from these smeared profiles increases from 7.9 to 9.0 nm and then to 13.5 nm as the length of the diblock increases (Table 1). The primary peak has a diffuse, small peak at a higher angle and for the 20//40 diblock, perhaps also a very weak third-order peak which becomes more distinct for the 40//40 system. The presence of additional peaks sug-

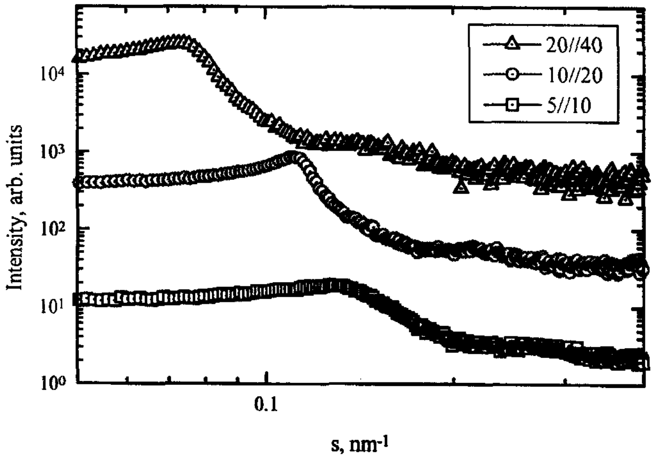

FIG. 2. Logarithmic plot of smeared SAXS intensity from 90% quaternized diblocks with increasing M_n at a BZ:DMAE ratio of 1:2. The curves are offset by a constant factor.

gests a longer-range ordered structure such as particles on a uniform lattice. The precursor diblocks show no small angle interference peaks, although there is a peak at about $s = 0.8\ \text{nm}^{-1}$ present in every diblock, quaternized or not (Figs. 5 and 6, discussed later). The peak at $0.8\ \text{nm}^{-1}$ is speculated to be due to intrachain correlation scattering from the benzyl moiety and is similar to the scattering peak (*d* ca. 1 nm) due to the repeat unit identity period of isotactic PS [12]. The identity period of the BZ chain should be larger than PS, since the BZ sidegroup is bulkier than the phenyl sidegroup of PS.

The effect of increasing the size of the nonionic block in the diblock while maintaining the size of the DMAE block is shown in Fig. 3. The peak intensity increases as the length of the nonionic block length increases, which suggests that the increase in intensity is due to either greater phase separation and/or an increase in the amount of long range order. It is thought that the amount of long range order is increased by increasing the length of the nonionic block. The 40//40 material may have a lamellar or cylindrical morphology, as it has a primary peak and two identifiable shoulders at estimated interdomain spacings of ca. $d_1/2$ and $d_1/3$. Note that the peaks move to lower angles (higher spacings) as the size of the nonionic block increases, as in Fig. 2. Though the length of the ionic block is the same, the estimated interdomain spacing increases from 11.3 to 13.5 and then to 29.9 nm as the DP_n of the BZ block goes from 10 to 20 to 40. This suggests that the BZ phase is a dispersed spheroid phase in at least the 10//40 system. A spheroid phase is assumed from the low volume fraction of the nonionic block in the 10//40 material. On the other hand, Venkateshwaran and coworkers [13] found that only 5 vol% of ionized endblocks in a diblock ionomer (synthesized anionically from methacrylates) exhibited dispersed cylinder morphology by TEM. The 20//40 material exhibits a strong secondary peak, indicating ionic cylinders or lamellae; the estimated *d*-spacings, determined from the smeared intensity, are ca. 2:1.

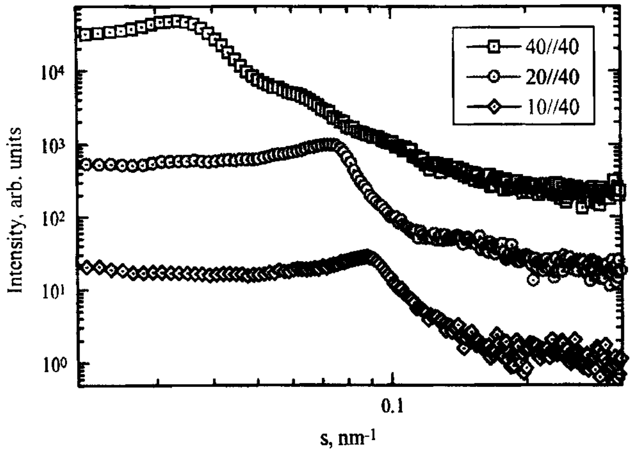

FIG. 3. Logarithmic smeared SAXS of diblocks of variable BZMA block length at constant DMAE ionic block length. The curves are offset by a constant factor.

Effect of Extent of Amine Salt Formation on Morphology

Figure 4 illustrates the effect of quaternization on the WAXD profile of a 20//20 BZ//DMAE diblock. In this figure the raw intensity in counts/second is plotted as a function of the scattering variable, *s*. Only the 20//20 diblock WAXD profiles are shown to illustrate the effect since the trend is similar for all ionomers. That is, the peak at $s \sim 0.8$ nm^{-1} ($d \sim 1.2$ nm, also seen in SAXS) strongly decreases in intensity as the extent of quaternization increases. The peak at $s \sim 2$ nm^{-1} ($d \sim 0.5$ nm) broadens upon quaternization but does not diminish or move. This strongly indicates that the latter peak is from inter- and intramolecular correlations in the BZ block, as mentioned before. The peak at $s \sim 0.8$ nm^{-1} is still visible in the SAXS profile (Fig. 5), and remains in the WAXD profile (but is weak) in the case of the 90 mol% sample.

While a speculation, the $s \sim 0.8$ nm^{-1} peak is likely from intrachain correlations between the dimethylamino sidegroups in the DMAE domains. This scattering is diminished in the formation of the quaternized phase, which utilizes the dimethylamino groups' unpaired electrons. The effect of the extent of quaternization on the morphology of two symmetric diblocks is illustrated in Figs. 5 (20//20 diblock) and 6 (40//40 diblock). In Fig. 5, as the DMAE block is further quaternized, the order in the system increases significantly. The precursor diblock shows a weak, broad scattering peak at $s \sim 0.8$ nm^{-1}, noted earlier. The additional peaks in the 30% systems are evidence of a higher degree of phase separation and phase contrast. The peaks move to higher "*s*" as the quaternization increases, and the peaks sharpen. It is believed that the 20//20 diblock system is lamellar, since the peak spacings scale as ca. s_1, $2s_1$, and $3s_1$. The 40//40 SAXS profiles (Fig. 6) are much like those for the 20//20 diblock, but the scattering is more intense. The ratio of the smeared spacings (Table 1) again suggest a lamellar morphology, as in the 20//20 ionomer. The characteristic peak at higher angles is present in all these ionomers, as mentioned above. Structural development due to ionization in both symmetric diblock follows the

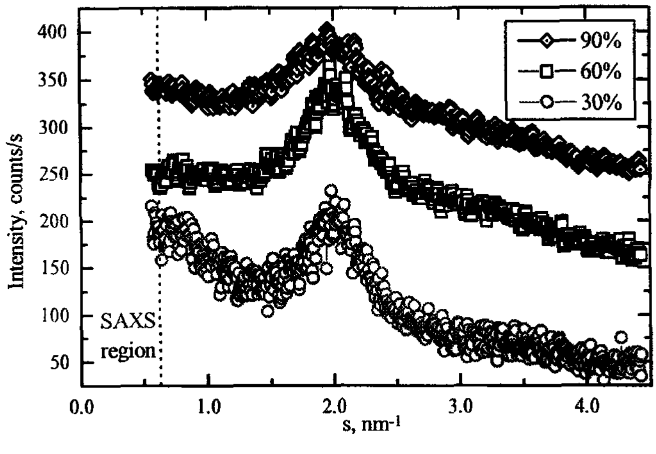

FIG. 4. Effect of quaternization on wide-angle diffraction characteristics of the 20//20 BZ//DMAE diblocks. The curves are offset by a constant vertical factor.

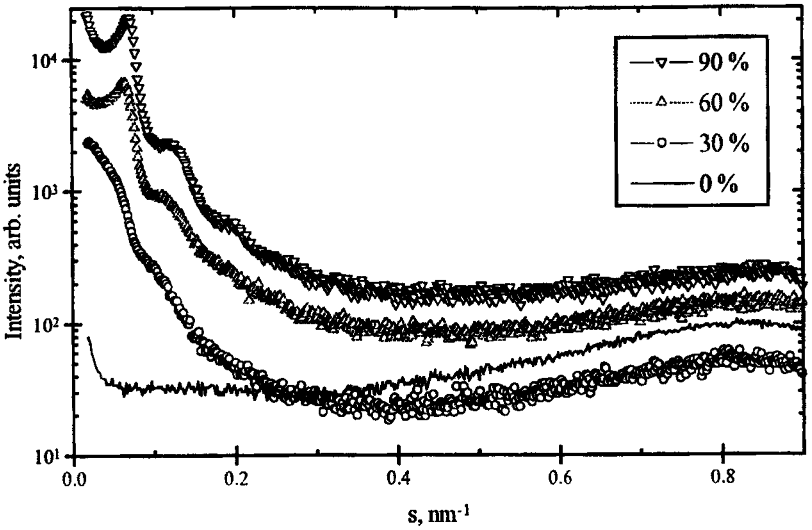

FIG. 5. Smeared SAXS of 20//20 BZ//DMAE diblock ionomers showing the effect of quaternization. Numbers refer to mol% DMAE quaternization. A constant offset factor has been used.

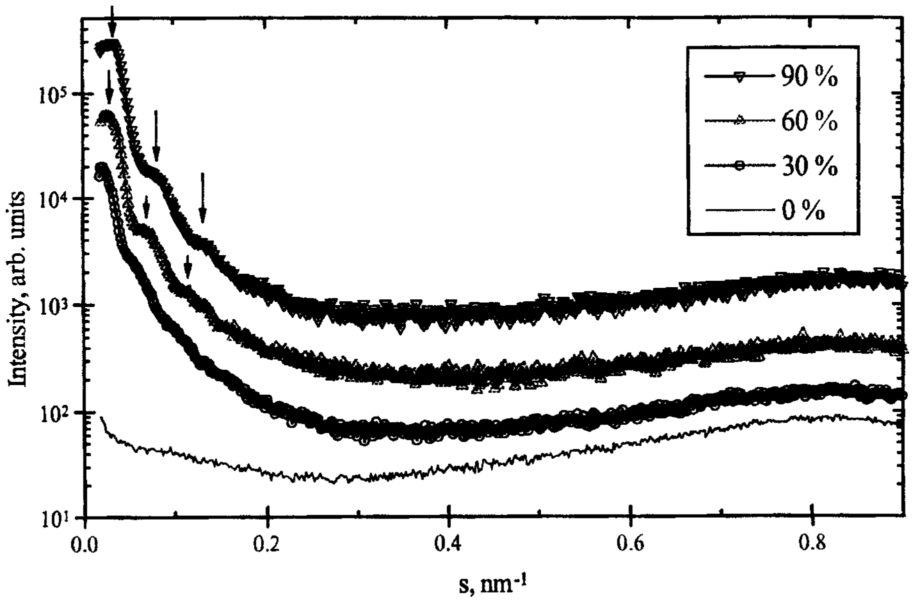

FIG. 6. Smeared SAXS of 40//40 BZ//DMAE diblock ionomers showing the effect of quaternization. Numbers refer to mol% DMAE quaternization. A constant offset factor has been used.

general process predicted by Marko and Rabin [14] in their model of the phase behavior of diblocks with one charged block. They predicted that the initial, small amount of ionization results in a dramatic increase in the value of χ^*N, the critical interaction parameter, so that phase separation occurs. At low degrees of ionization, a structurally "coarse" phase separation occurs; at higher degrees of ionization an extended structure (on increasingly smaller length scales) develops. It can be seen in Figs. 5 and 6 that quaternization initially results in a broad peak like that generally observed in phase separated systems. At higher amounts of quaternization, the extended structure itself is registered at smaller length scales as secondary maxima. The development of extended structure results in a slight shift in the primary scattering peak (arrows in Fig. 6), but the majority of the phase separation is already complete at 30 mol% quaternization, and the structure continues to develop up to 90 mol%. Although SAXS shows much about the structure and its development, TEM was also employed to clarify the structure of the symmetric systems.

Transmission Electron Microscopy

Figure 7 shows a typical TEM from the 40//40 ionomer materials examined by SAXS in the prior section. The texture of the morphology appears to be that of ellipsoidal vesicles of BZ interpenetrated by a matrix of quaternized DMAE, and the BZ domains appear to be arranged in rows in a few regions. In this micrograph the domains are ca. 40 nm in length and 15 nm in diameter, with a center-to-center distance of about 20–25 nm. Because of the large variation in the structural features noted from the micrographs, these numbers are only approximate. The interdomain spacing of 30 nm from SAXS in Table 1 agrees well with the general center-to-center distance from TEM. However, it is still interesting that such an apparently disordered morphology can give rise to distinctive SAXS peaks similar to a lamellar system. On the other hand, the cutting direction in highly ordered systems can dramatically influence the micrograph. For example, Feng and coworkers studied segmented ionenes based on PTMO soft segments and benzyl dihalide hard segments in which the highly ordered cylindrical ionic domains appeared more like disordered blotches when viewed parallel to the cylinder axes [15].

Figure 8 shows a typical TEM for the 40//40 diblock material, but cast from a 10 wt% solution which clearly shows the presence of spheroid BZ domains in a darker DMAE matrix. This shows that a more dilute solution allows the diblocks to organize in a micellar fashion. As discussed previously, Luzzati et al. found that a concentrated solution of surfactant had a cylindrical structure, and a dilute solution gave spheres. This was attributed to the micellization effect and overlap of the micelles at higher concentration. In the case at hand, these cylindrical and lamellar structures are observed in the solid state and not in the solution itself. Thus, the symmetric diblock ionomers are likely not purely lamellar in texture, but possess some cylindrical BZ domains and may exhibit "perforated," catenoid lamellae, as has been observed by several groups [16] in higher M_n SB diblocks containing homopolymer-PS.

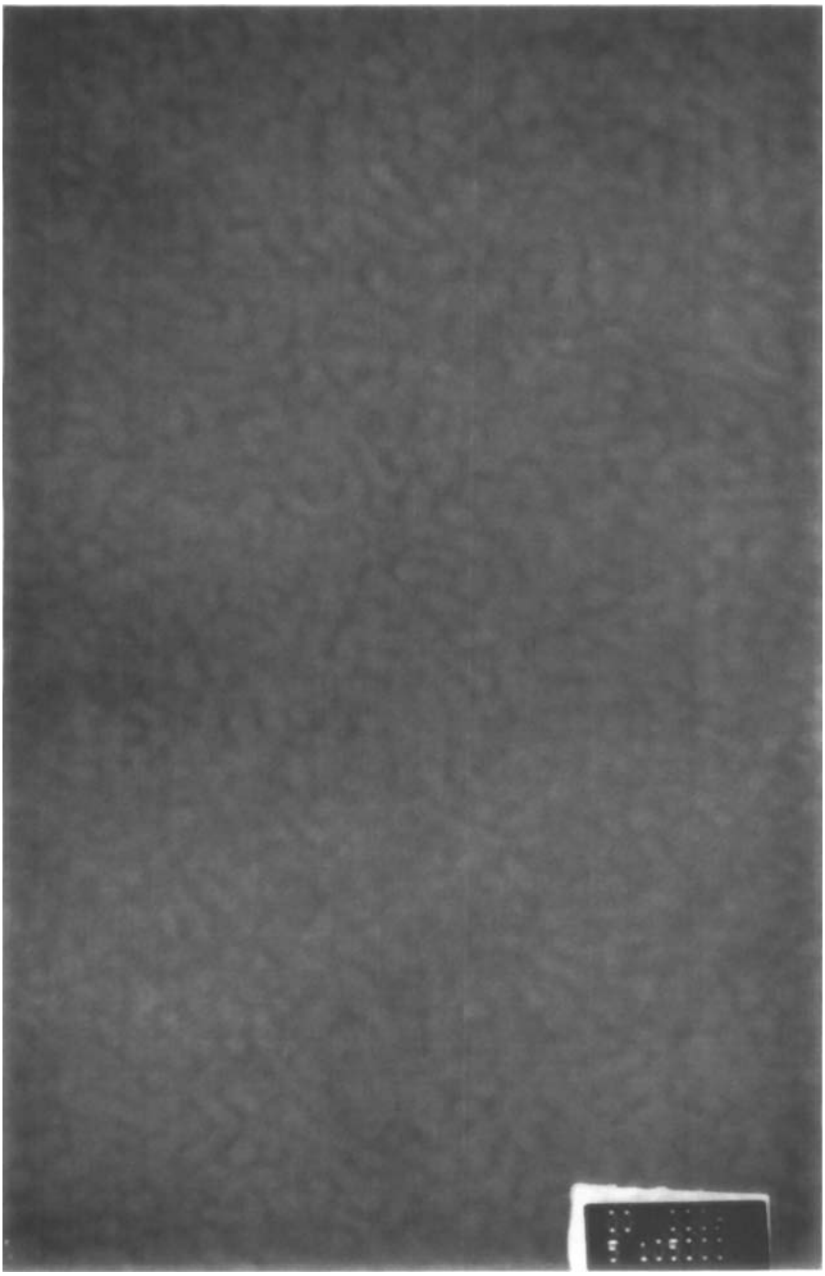

FIG. 7. TEM of 40//40 ionomer, 30 wt% cast film.

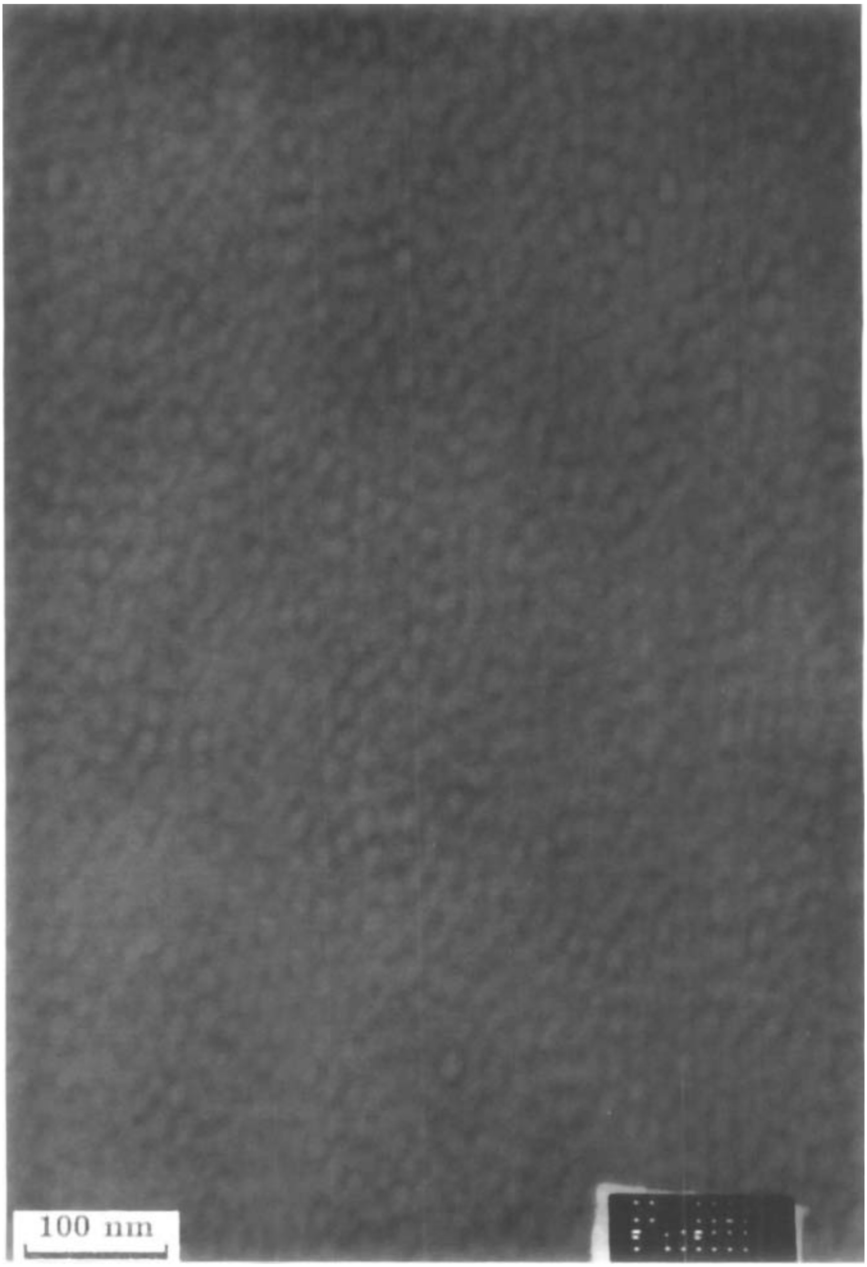

FIG. 8. TEM of 40//40 ionomer, 10 wt% cast film.

CONCLUSIONS

Low M_n diblock copolymers in a disordered melt initially form highly ordered structures when one block is ionized due to a strong tendency to microphase separate. SAXS indicates that even small diblocks organize into ordered structures upon ionization, and that larger, more symmetric diblocks form near lamellar textures, also observed in TEM. Ionization initially results in phase separation and later in perfection of the ordered, phase-separated structure of the final state. In smaller diblocks it is apparent that the ordered structure is less developed than in those with higher M_ns, as implied by a lack of secondary SAXS scattering maxima. Finally, the micellization process in solution appears to strongly affect the final morphology. At lower concentrations there is no micellar overlap and spherical dispersed domains are seen, whereas elongated domains at higher concentrations tend to stack into ordered structures, forming the lamellar texture.

ACKNOWLEDGMENTS

D.L. thanks C. S. Hutchins for a summer research internship, H. Spinelli for the polymers and the DuPont Company which made this research possible, Mr. Steve McCartney for TEM, and Mr. Watson Srinivas for WAXD assistance.

REFERENCES

[1] (i) O. W. Webster, W. B. Farnham, and D. Y. Sogah, Eur. Patent 0 068 887 (1987). (ii) O. W. Webster, W. R. Hertler, D. Y. Sogah, W. B. Farnham, and T. V. Rajan Babu, *J. Am. Chem. Soc.*, *105*, 5706 (1983). (iii) O. W. Webster, W. R. Hertler, D. Y. Sogah, W. B. Farnham, and T. V. Rajan Babu, *J. Macromol. Sci.—Chem.*, *A21*, 943 (1984).

[2] T. P. Davis, D. M. Haddleton, and S. N. Richards, *J. Macromol. Sci.—Rev. Macromol. Chem. Phys.*, *C34*(2), 243 (1994).

[3] G. C. Eastmond and O. W. Webster, in *New Methods of Polymer Synthesis*, Vol. 22 (J. R. Ebdon, Ed.), Blackie, 1991.

[4] K. Hatada and T. Kitayama, Japanese Patent 01 90 209 (1987).

[5] O. W. Webster and D. Y. Sogah, in *Recent Advances in Mechanistic and Synthetic Polymerisation* (M. Fontille and A. Guyot, Eds.), (NATO ASI Series No. C215, p. 3), D. Reidel, Dordrecht, 1987.

[6] J. A. Simms and H. J. Spinelli, *J. Coatings Technol.*, *59*, 125 (1987).

[7] R. Asami, M. Takaki, and Y. Moriyama, *Polym. Bull.*, *16*, 125 (1986).

[8] H. J. Spinelli, in *Progress in Pacific Polymer Science* (P. C. Anderson and Y. Imanishi, Eds.), Springer-Verlag, Berlin, 1991, p. 249.

[9] (i) F. Husson, *Compt. Rend.*, *253*, 2948 (1961). (ii) F. Reiss-Husson and V. J. Luzzati, *J. Phys. Chem.*, *68*, 3504 (1964). (iii) F. Reiss-Husson and V. J. Luzzati, *J. Colloid Interface Sci.*, *21*, 534 (1966). (iv) V. J. Luzzati, in *Biological Membranes* (D. Chapman, Ed.), Academic Press, New York, NY, 1968, p. 71.

[10] M. H. F. Wilkins, A. E. Blaurock, and D. M. Engelman, *Nature New Biol.*, *230*, 72 (1971).

[11] (i) A. G. Lee, *Biochim. Biophys. Acta, 472*, 237 (1977). (ii) A. G. Lee, *Ibid.*, *472*, 2285 (1977).

[12] L. Alexander, *X-ray Diffraction Methods in Polymer Science*, 1985, p. 365.

[13] L. N. Venkateshwaran, G. A. York, C. D. DePorter, J. E. McGrath, and G. L. Wilkes, *Polym. Prepr.*, *30*(2), 105 (1989).

[14] J. F. Marko and Y. Rabin, *Macromolecules, 25*, 1503 (1992).

[15] D. Feng, G. L. Wilkes, C. M. Leir, and J. E. Stark, *J. Macromol. Sci.—Chem.*, *A26*(8), 1151 (1989).

[16] (i) M. M. Disko, K. S. Liang, S. K. Behal, R. J. Roe, and K. J. Jeon, *Macromolecules, 26*, 2983 (1993). (ii) R. J. Spontak, S. D. Smith, and A. Ashraf, *Ibid.*, *26*, 956 (1993). (iii) T. Hashimoto, S. Koizumi, H. Hasegawa, T. Izumitani, and S. T. Hyde, *Ibid.*, *25*, 1433 (1992). (iv) E. L. Thomas, D. M. Anderson, C. S. Henkee, and D. Hoffman, *Nature, 334*, 598 (1988).

Received July 21, 1996
Revision received September 1, 1996